Available online at www.sciencedirect.com
SCIENCE DIRECT®
Journal of Sound and Vibration 287 (2005) 939–960
JOURNAL OF SOUND AND VIBRATION
www.elsevier.com/locate/jsvi

Parameter estimation of unstable, limit cycling systems using adaptive feedback linearization: example of delta wing roll dynamics

Himani Jain, Vivek Kaul, N. Ananthkrishnan*

Department of Aerospace Engineering, Indian Institute of Technology Bombay, Mumbai 400076, India

Received 11 May 2004; received in revised form 16 November 2004; accepted 9 December 2004
Available online 17 February 2005

Abstract

The problem of estimating the unknown parameters of a nonlinear (plant) model for an unstable, limit cycling system is considered. A feedback linearizing control is used that aims to cancel the nonlinear terms in the plant model and to alter the linear terms such that the closed-loop plant model matches with a specified linear reference model. The controller parameters are unknown and are evolved, starting from zero, by an adaptive law that aims to drive them towards their ideal values that would provide perfect model matching between the reference model and the closed-loop plant model. The converged controller parameters would then provide good estimates for the unknown plant parameters. An external forcing signal is considered, common to both the reference model and the plant, and an adaptation law in the presence of this forcing function is derived using Lyapunov methods. Significantly, the same stability analysis is used both to derive a controller for the limit cycling system and also to provide a solution to the problem of parameter estimation. Simulations using an exponentially decaying sinusoidal forcing show that good estimates of the linear plant parameters are obtained for a wide range of values of the amplitude, frequency, and decay time of the forcing function, and also in the presence of measurement noise in the plant output. The problem of non-convergence of the nonlinear controller parameters is examined in some detail. The parameter estimation method is demonstrated in our paper on a nonlinear model for a rolling delta wing; however, it should be equally applicable to a wide class of limit cycling systems modeled by a set of nonlinear differential equations.

*Corresponding author. Tel.: +91 22 25767130; fax: +91 22 25722602.
E-mail address: akn@aero.iitb.ac.in (N. Ananthkrishnan).

0022-460X/$ - see front matter © 2005 Elsevier Ltd. All rights reserved.
doi:10.1016/j.jsv.2004.12.013

1. Introduction

Self-excited oscillations called limit cycles are commonly observed in a wide variety of nonlinear systems [1]. In mechanical systems, limit cycles usually arise as a result of loss of damping at a particular equilibrium state [2,3]. The undamped equilibrium state is then unstable and the system, in response to a small perturbation, settles into an oscillation about the unstable equilibrium state with constant amplitude and frequency, which are characteristic of the limit cycle.

The problem of modeling the nonlinear function that best represents the limit cycle dynamics is part of a broader class of problems called nonlinear system identification and is an extremely challenging task [4,5]. However, for many nonlinear systems of engineering interest that display limit cycle behavior, such as the delta wing roll dynamics considered in this paper, the structure of the nonlinear function is known and it is only the parameters in the nonlinear function that are unknown or uncertain. The problem then reduces from one of system identification to that of estimating the unknown or uncertain parameters for a given system model from experimentally measured data.

The parameter estimation problem for nonlinear systems is itself not a particularly simple problem to solve. First of all, even for a single dof system, the number of parameters can be considerably larger than the number of state variables and it may not be possible to estimate all the parameters simultaneously. Secondly, there is an inherent contradiction between the nature of the system response required to estimate the linear parameters (ones that appear in the coefficients of terms that are linear in the state variables) as against that required for the estimation of the nonlinear parameters. Linear parameters are best estimated when the system shows small-amplitude response near the equilibrium state; in this case, the nonlinear terms in the model are numerically less significant as compared to the terms that contain the linear parameters. On the other hand, good estimates of the nonlinear parameters are obtained only when the system shows large-amplitude response. There is a third additional complication in case of unstable systems; these systems have to be operated in closed loop with a controller in place in order to restrict potentially dangerous, large excursions in system response. In that case, while the parameters of the open-loop system are the ones that need to be estimated, only the system closed-loop response can be measured. In fact, attempts to adequately excite the system response may be suppressed by the controller, making it difficult to acquire sufficiently rich measured data and hence to effectively estimate the parameters [6].

One potentially effective solution to the problem of parameter estimation in case of unstable systems is to use an adaptive scheme with some form of feedback linearization-based controller. As pointed out in Ref. [7], such systems are usually required to satisfy the following conditions: (i) The nonlinear plant dynamics can be linearly parameterized; (ii) the full state is measurable; and (iii) nonlinearities can be canceled stably (i.e., without unstable hidden modes or dynamics) by the control input if the parameters are known. Many simple systems of engineering interest do in fact satisfy these conditions, and thus adaptive schemes have been used for control and estimation of unstable systems in practice. Control of limit cycle oscillations in an unstable system satisfying conditions (i)–(iii) above has been carried out in Refs. [8,9] using an adaptive feedback linearization strategy. Both [8,9] considered the problem of limit cycle oscillations in the roll dynamics of aircraft with a delta wing, a phenomenon called wing rock [10]. Adaptive feedback

linearization, along the lines of Ref. [8], has also been practically applied to an experimental delta wing model in a wind tunnel, and control of wing rock limit cycles has been successfully demonstrated [11].

The main ingredients of an adaptive feedback linearization scheme can be summarized as follows: (1) An experimental or a mathematical model of the nonlinear system dynamics (also called the plant), assuming the model to be linearly parameterized. All the plant state variables x_p are assumed to be measurable, although in Ref. [11] only one of the two plant states was physically measured, the other being obtained by suitably operating on the measured signal. (2) A feedback linearization-based controller that is linearly parameterized by a parameter vector θ. When θ is correctly chosen to be a particular value θ^*, the controller eliminates the nonlinear terms in the plant dynamics, making the combined plant-controller dynamics in the closed-loop linear and exactly identical to the reference model [see (3) below]. (3) A reference model, usually linear, stable, and of the same order as the nonlinear plant model; the reference model states x_m are expected to be tracked by the plant states x_p. (4) An adaptation mechanism that evolves the controller parameters θ as per a specified law with the aim of driving the error e between the plant states x_p and the reference model states x_m to zero.

It must be recognized that there are three facets to the adaptive feedback linearization problem discussed above. (1) Regulating the plant state variables x_p to the unstable equilibrium state x_p^*, called the control problem. (2) Making the plant states x_p follow the reference model states x_m, or driving the error e between them to zero, called the tracking problem. (3) Having the controller parameters θ converge to that special value θ^* which makes the closed-loop plant-controller system identical to the reference model, called the parameter convergence problem. In this case, subtracting the known reference model parameters from the converged value θ^* of the controller parameters gives an estimate of the unknown or uncertain open-loop plant parameters.

For problems involving only control of an unstable, limit cycling system using an adaptive feedback linearization scheme, both tracking and regulation can be successfully achieved even in the absence of parameter convergence. In fact, it is well known that parameter convergence requires the use of external forcing with an additional property called *persistent excitation* that needs to be satisfied [12]. Unfortunately, sufficient conditions for parameter convergence in case of nonlinear plant models are generally unavailable and hence the persistent excitation condition can rarely be checked a priori [13]. Consequently, it is not always possible to guarantee a satisfactory solution to the parameter estimation problem for unstable, limit cycling systems, and therefore the question of parameter convergence in adaptive schemes as applied to nonlinear systems has attracted much attention recently [14].

Unstable, limit cycling systems are frequently encountered in engineering practice, and there is considerable interest in the problem of parameter estimation for such systems, e.g., aircraft [15], combustion chambers [16]. While adaptive feedback linearization schemes have been used for control of limit cycling systems, there is no reference in the literature to their having been successfully employed for parameter estimation of nonlinear models undergoing limit cycle oscillations. For the problem of delta wing roll dynamics discussed earlier, [8,11] limited themselves to the tracking and control problem, and did not address the question of parameter estimation. Parameter convergence was not explicitly considered in Ref. [9] either, though parameter estimates obtained in the course of the computations have been reported; four of the five parameters reported did not converge to the correct values and the one that did converge was

a constant term in the nonlinear model. In fact, none of these formulations included an external excitation and hence, in the light of the above discussion, parameter convergence was not to be expected. This background provides us with the motivation to consider the problem of parameter estimation of an unstable, limit cycling system, using a nonlinear model for the limit cycling delta wing as an example.

In the following sections of this paper, the nonlinear model for the delta wing roll dynamics is first briefly described, followed by the feedback linearizing control law, the closed-loop plant dynamics, and the reference model dynamics. The adaptation law is then derived using Lyapunov methods, and conditions for stability of the closed-loop system are verified. Using a forcing function of the form suggested by the stability analysis, the closed-loop plant dynamics with the adaptation law is simulated and the problem of parameter convergence is examined. The results are contrasted with the unforced case, where parameter convergence is not obtained. Parametric studies are carried out by varying the amplitude, frequency, and decay time of the forcing function. Finally, measurement noise is included in the simulation to check whether parameter convergence is still achieved in a noisy environment.

2. Nonlinear model and open-loop response

A nonlinear model for the limit cycle dynamics of the delta wing has been given in Ref. [17], as follows

$$\begin{aligned}\dot{x}_{p_1} &= x_{p_2},\\ \dot{x}_{p_2} &= c_1 a_1 x_{p_1} + (c_1 a_2 - c_2) x_{p_2} + c_1 a_3 x_{p_1}^3 + c_1 a_4 x_{p_1}^2 x_{p_2} + c_1 a_5 x_{p_1} x_{p_2}^2 + d_0 u,\end{aligned} \tag{1}$$

where c_1, c_2 are constants with the following values: $c_1 = 0.354$, $c_2 = 0.001$; a_1 through a_5 are the five unknown parameters that need to be estimated, d_0 is assumed to be known, and u is the control input to the model. The overdots denote differentiation with respect to a nondimensional time; thus, every term in Eq. (1) is dimensionless.

Note that the model in Eq. (1) is slightly different from those considered in the adaptive feedback linearization studies in Refs. [8,9]; both those models were taken from Ref. [10] and contained nonanalytical terms as well as a constant term. In addition, Monahemi and Krstic [9] ignored the cubic term in x_{p_1}. It has been shown in Ref. [18] that the model in Eq. (1) taken from Ref. [17] is more accurate than those used in previous studies [8,9], as well as easier to analyze since it does not contain nonanalytical terms.

The mathematical model of the plant, Eq. (1), is simulated by using the following values of the parameters a_1 through a_5 obtained from the experimental work of Levin and Katz [19], and reported in Ref. [17]: $a_1 = -0.05686$, $a_2 = 0.03254$, $a_3 = 0.07334$, $a_4 = -0.3597$, $a_5 = 1.4681$. The open-loop response of the nonlinear system, Eq. (1), to an initial perturbation of $x_{p_1}(0) = 0.4$, $x_{p_2}(0) = 0$, with no control applied, i.e., $u = 0$, is as shown in Fig. 1. Clearly, both variables, x_{p_1} and x_{p_2}, show limit cycle dynamics with constant amplitude and frequency. Repeated simulation for a variety of initial conditions, with $u = 0$ in every case, shows, as expected, the amplitude and frequency of the limit cycle motion to be independent of the initial perturbation.

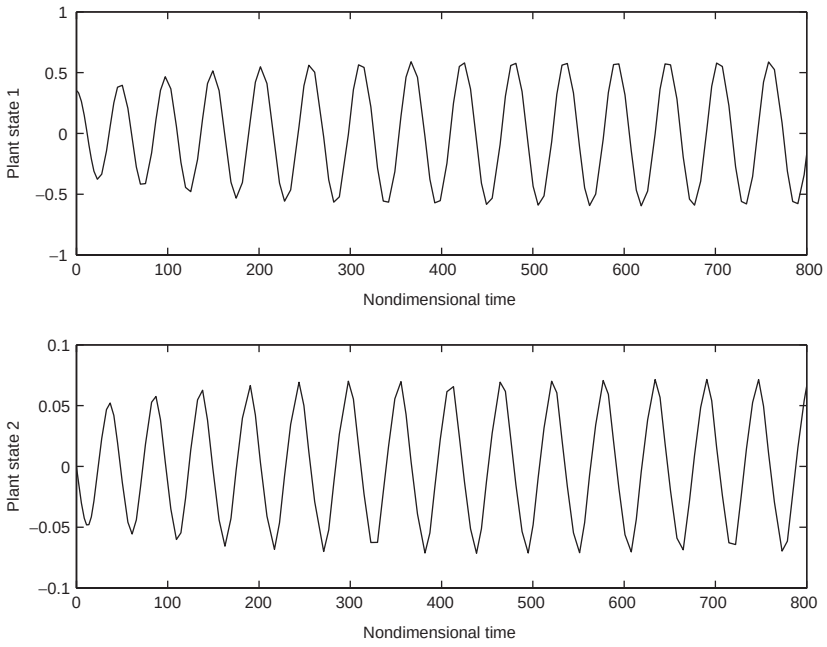

Fig. 1. Open-loop response of nonlinear system, Eq. (1), for initial perturbation $(x_{p_1}(0), x_{p_2}(0)) = (0.4, 0)$ and no control $(u = 0)$, showing limit cycle oscillations in x_{p_1} and x_{p_2}.

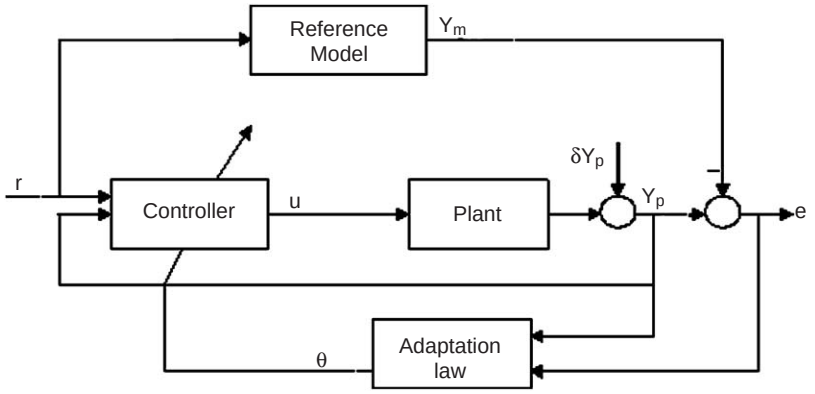

Fig. 2. Block diagram of adaptive feedback linearization scheme.

3. Adaptive feedback linearization scheme

A block diagram of the adaptive feedback linearization scheme is shown in Fig. 2. The nonlinear plant dynamics is modeled as given in Eq. (1). Both the plant states, x_{p_1}, x_{p_2}, are assumed to be measurable; however, the measurements, y_{p_1}, y_{p_2}, are assumed to be corrupted by

measurement noise, $\delta y_{p_1}, \delta y_{p_2}$, as follows

$$y_{p_1} = x_{p_1} + \delta y_{p_1},$$
$$y_{p_2} = x_{p_2} + \delta y_{p_2}. \tag{2}$$

The measurement noise, $\delta y_{p_1}, \delta y_{p_2}$, are taken to be small-amplitude high-frequency signals as recommended in Ref. [7]. Measurement noise was not considered in either of Refs. [8,9]; however, the experimental work in Ref. [11] suggests that the adaptive feedback linearization approach is effective in the presence of measurement noise.

The feedback linearizing control is chosen to be of the following form:

$$u = -(\theta_1 y_{p_1} + \theta_2 y_{p_2} + \theta_3 y_{p_1}^3 + \theta_4 y_{p_1}^2 y_{p_2} + \theta_5 y_{p_1} y_{p_2}^2) + r(t), \tag{3}$$

where $\theta_1, \ldots, \theta_5$ are the controller parameters that need to be adapted as they cannot be determined a priori in the absence of knowledge of the plant parameters, $a_1, \ldots, a_5$. The term $r(t)$ denotes an external forcing function that is necessary, as discussed earlier, to ensure that the persistent excitation condition is satisfied for parameter convergence to take place.

The combined plant-controller system can now be written by using the control law, Eq. (3), in the mathematical model for the plant, Eq. (1), as follows:

$$\dot{x}_{p_1} = x_{p_2},$$
$$\dot{x}_{p_2} = (c_1 a_1 - d_0\theta_1)x_{p_1} + (c_1 a_2 - c_2 - d_0\theta_2)x_{p_2} + (c_1 a_3 - d_0\theta_3)x_{p_1}^3 + (c_1 a_4 - d_0\theta_4)x_{p_1}^2 x_{p_2} + (c_1 a_5 - d_0\theta_5)x_{p_1} x_{p_2}^2 + d_0 r(t) + [\text{terms in } \delta y_{p_1}, \delta y_{p_2}]. \tag{4}$$

The terms in $\delta y_{p_1}, \delta y_{p_2}$ have not been spelt out in Eq. (4) as they are not considered for the analysis of the adaptive feedback linearization scheme. However, they are included in the simulation of the closed-loop system with the adaptation law to be presented later.

First- or second-order models for the sensor and/or actuator dynamics may be included, if desired. A first-order actuator dynamics model has been considered in Ref. [9]; however, no significant increase in the complexity of the analysis is noticed, nor are the results of the adaptive control scheme any different, due to the addition of the actuator dynamics model. Hence, neither sensor nor actuator dynamics has been explicitly modeled in the present work.

The reference model is taken to be a second-order linear system as follows

$$\dot{x}_{m_1} = x_{m_2},$$
$$\dot{x}_{m_2} = -\omega_n^2 x_{m_1} - 2\zeta\omega_n x_{m_2} + d_0 r(t). \tag{5}$$

The reference model parameters, ζ, ω_n, are constants, and are chosen to have the following values in dimensionless units: $\zeta = 0.707$, $\omega_n = 0.1$. The forcing function $r(t)$ used to excite the reference model is the same as that used in Eq. (3). For the reference model, the outputs, y_{m_1}, y_{m_2}, are identical to the states, as below

$$y_{m_1} = x_{m_1},$$
$$y_{m_2} = x_{m_2}. \tag{6}$$

Comparing Eqs. (4) and (5), the combined plant-controller dynamics will be exactly identical to the reference model dynamics (but for the presence of measurement noise in the plant dynamics),

if the following equalities hold:

$$\begin{aligned} c_1a_1 - d_0\theta_1^* &= -\omega_n^2, \\ c_1a_2 - c_2 - d_0\theta_2^* &= -2\zeta\omega_n, \\ c_1a_3 - d_0\theta_3^* &= 0, \\ c_1a_4 - d_0\theta_4^* &= 0, \\ c_1a_5 - d_0\theta_5^* &= 0, \end{aligned} \tag{7}$$

where $\theta_1^*, \ldots, \theta_5^*$ are the ideal controller parameter values for which the control law, Eq. (3), theoretically provides the possibility of perfect model matching between the plant-controller dynamics and the reference model dynamics. In practice, if the adaptation law succeeds in evolving the controller parameters to a sufficiently good approximation to their ideal values, $\theta_1^*, \ldots, \theta_5^*$, then Eq. (7) could be used to estimate the plant parameters, $a_1, \ldots, a_5$.

3.1. Output error and parameter error

The tracking error between the plant and reference model outputs is defined as follows

$$\begin{aligned} e_1 &= y_{p_1} - y_{m_1}, \\ e_2 &= y_{p_2} - y_{m_2}. \end{aligned} \tag{8}$$

The error dynamics can then be shown to satisfy the following equations by using Eqs. (4) and (2) for the plant dynamics, and Eqs. (5) and (6) for the reference model dynamics

$$\begin{aligned} \dot{e}_1 &= e_2 + [\text{terms in } \delta y_{p_1}, \delta y_{p_2}], \\ \dot{e}_2 &= -\omega_n^2 e_1 - 2\zeta\omega_n e_2 + (c_1a_1 - d_0\theta_1 + \omega_n^2)x_{p_1} + (c_1a_2 - c_2 - d_0\theta_2 + 2\zeta\omega_n)x_{p_2} \\ &\quad + (c_1a_3 - d_0\theta_3)x_{p_1}^3 + (c_1a_4 - d_0\theta_4)x_{p_1}^2 x_{p_2} + (c_1a_5 - d_0\theta_5)x_{p_1}x_{p_2}^2 + [\text{terms in } \delta y_{p_1}, \delta y_{p_2}]. \end{aligned} \tag{9}$$

Using the definitions in Eq. (7) for the θ_i^*, and defining the error in the controller parameters, η_i, in the following manner:

$$\eta_i = \theta_i^* - \theta_i, \quad i = 1, \ldots, 5. \tag{10}$$

Eq. (9) for the output error dynamics can be rewritten as follows

$$\begin{aligned} \dot{e}_1 &= e_2 + [\text{terms in } \delta y_{p_1}, \delta y_{p_2}], \\ \dot{e}_2 &= -\omega_n^2 e_1 - 2\zeta\omega_n e_2 + d_0\eta_1 x_{p_1} + d_0\eta_2 x_{p_2} + d_0\eta_3 x_{p_1}^3 \\ &\quad + d_0\eta_4 x_{p_1}^2 x_{p_2} + d_0\eta_5 x_{p_1}x_{p_2}^2 + [\text{terms in } \delta y_{p_1}, \delta y_{p_2}]. \end{aligned} \tag{11}$$

Note that the forcing function $r(t)$ does not appear in the equation for the error dynamics.

3.2. Adaptation law

The adaptation law is derived under the condition of no measurement noise. The derivation is similar to that outlined in Ref. [8]; however, the present derivation also considers the effect of the forcing function that was not included in Ref. [8]. Since the forcing function $r(t)$ does not enter

into the error dynamics, Eq. (11), it becomes necessary to additionally consider the plant dynamics, Eq. (4), in the analysis to derive the adaptation law.

The error dynamics, Eq. (11), is first compactly represented as follows

$$\begin{pmatrix} \dot{e}_1 \\ \dot{e}_2 \end{pmatrix} = \begin{bmatrix} 0 & 1 \\ -\omega_n^2 & -2\zeta\omega_n \end{bmatrix} \begin{pmatrix} e_1 \\ e_2 \end{pmatrix} + \begin{pmatrix} 0 \\ 1 \end{pmatrix} d_0 \eta^{\mathrm{T}} h(x_p) \tag{12}$$

or

$$\dot{e} = Ae + bd_0\eta^{\mathrm{T}} h(x_p), \tag{13}$$

where $e^{\mathrm{T}} = (e_1, e_2)$ is the vector of output errors, A is the 2×2 matrix in Eq. (12), $b^{\mathrm{T}} = (0, 1)$, η is the vector of parameter errors, $x_p^{\mathrm{T}} = (x_{p_1}, x_{p_2})$, and $h(x_p)$ is the vector given by

$$h^{\mathrm{T}}(x_p) = (x_{p_1}, x_{p_2}, x_{p_1}^3, x_{p_1}^2 x_{p_2}, x_{p_1} x_{p_2}^2).$$

Note that the evolution of the error as given by Eq. (13) depends on the error e itself, the parameter error η, and a function of the plant states $h(x_p)$; symbolically, $\dot{e} = f_e(e, \eta, x_p)$.

In a like manner, the closed-loop plant dynamics, Eq. (4), can be written as follows

$$\dot{x}_p = Ax_p + bd_0\eta^{\mathrm{T}} h(x_p) + d_0 r(t), \tag{14}$$

which appears similar to the error dynamics, Eq. (13), but for the appearance of the forcing term, $r(t)$. Symbolically, this can be written as $\dot{x}_p = f_x(\eta, x_p, r(t))$.

An adaptation law of the form, $\dot{\eta} = g(e, x_p)$, is desired such that it drives the output error e, plant states x_p, and parameter error η, all to zero. Then, since $\eta = \theta^* - \theta$, and noting that the ideal parameters θ^* are taken to be time invariant, the parameter update law is obtained as $\dot{\theta} = -g(e, x_p)$. Note that the adaptation law for $\dot{\eta}$ cannot be a function of η as that would require the parameter update law for $\dot{\theta}$ to be a function of θ and θ^*, but the θ^* are unknown.

For the derivation of the adaptation law, the 9-D dynamical system consisting of the output error dynamics, $\dot{e} = f_e(e, \eta, x_p)$ in Eq. (13), the plant dynamics, $\dot{x}_p = f_x(\eta, x_p, r(t))$ in Eq. (14), and the parameter error dynamics, $\dot{\eta} = g(e, x_p)$, is considered. Note that this dynamical system is nonautonomous due to the presence of the forcing term $r(t)$ in the function f_x. Nevertheless, $(e, x_p, \eta) = (0, 0, 0)$ is an equilibrium point of this dynamical system provided $r(t) = 0$ for all $t \geqslant t_0$, for some $t_0 > 0$. It is of interest to determine the stability of this equilibrium point as that would establish tracking ($e = 0$), regulation ($x_p = 0$), and parameter convergence ($\eta = 0$) for the adaptive feedback linearization scheme. To this end, a time-invariant candidate Lyapunov function is chosen as follows

$$V(e, x_p, \eta) = e^{\mathrm{T}} P_e e + x_p^{\mathrm{T}} P_x x_p + d_0^2 \eta^{\mathrm{T}} \Gamma \eta, \tag{15}$$

where P_e, P_x are symmetric 2×2 matrices that are positive definite, and Γ is a diagonal 5×5 weighting matrix with all the diagonal entries, $\Gamma_1, \ldots, \Gamma_5$, positive, i.e., Γ is also a positive definite matrix. Consequently, it is easily checked that $V(0, 0, 0) = 0$, and $V(e, x_p, \eta) > 0$ for all other values of e, x_p, η; hence, $V(e, x_p, \eta)$ is a positive definite function with a minimum at $(e, x_p, \eta) = (0, 0, 0)$.

The adaptation law is derived by first computing $\dot{V}$, the derivative of the function V in Eq. (15) along the trajectory of Eqs. (13), (14), and (16), in 9-D space. Equating the sum of terms

containing $\dot{\eta}$ and $h(x_p)$ to zero gives the parameter error update law as follows

$$\dot{\eta} = -\frac{1}{d_0}\Gamma^{-1}h(x_p)(e^{\mathrm{T}}P_e + x_p^{\mathrm{T}}P_x)b \tag{16}$$

and the remaining terms in the expression for $\dot{V}$ are as below

$$\dot{V} = -e^{\mathrm{T}}Q_e e - x_p^{\mathrm{T}}Q_x x_p + 2(x_p^{\mathrm{T}}P_x b)d_0 r(t). \tag{17}$$

Q_e, Q_x in Eq. (17) are positive definite symmetric matrices and are related to the matrices P_e, P_x in Eq. (15) by the Lyapunov equation

$$A^{\mathrm{T}}P + PA = -Q \tag{18}$$

by virtue of A being a stable matrix. It has been shown [20] that it is adequate to select Q to be the identity matrix I, in which case the elements of the P matrix can be obtained by solving Eq. (18) as follows

$$\begin{aligned} p_{11} &= 2\zeta\omega_n p_{21} + \omega_n^2 p_{22}, \\ p_{12} = p_{21} &= \frac{1}{2\omega_n^2}, \\ p_{22} &= \frac{1/2 + p_{12}}{2\zeta\omega_n}. \end{aligned} \tag{19}$$

In the present study, the choice $Q_e = I$ is made, and hence the P_e matrix is as given in Eq. (19). Q_x is taken to be $\varepsilon^2 I$, with $\varepsilon = 0.1$; in this case, every element of P_x is obtained as $1/\varepsilon^2$ times the corresponding element p_{ij} in Eq. (19).

3.3. Stability analysis

First consider the case where $r(t) = 0$. It is then clear from Eq. (17) that $\dot{V} \leqslant 0$, i.e., $\dot{V}$ is a negative semi-definite function. Hence, V in Eq. (15) is indeed a valid Lyapunov function, and therefore the results of Lyapunov stability analysis are applicable to the present problem. It follows that the dynamical system with states e, x_p, η is globally stable, i.e., e, x_p, η are bounded. Consequently, Eqs. (13) and (14), respectively, show $\dot{e}$ and $\dot{x}_p$ to be bounded as well. It then follows that $\ddot{V}$, which can be obtained from Eq. (17), is bounded, and hence $\dot{V}$ is uniformly continuous. Use of Barbalat's lemma (refer [7, p. 125]) then assures us that $\dot{V} \to 0$ as $t \to \infty$, which implies, by reference to Eq. (17), that both $e \to 0$ and $x_p \to 0$ as $t \to \infty$. Thus, global asymptotic convergence of the output error e to zero and the plant states x_p to zero is established. However, note that the equilibrium point $(e, x_p, \eta) = (0, 0, 0)$ is not asymptotically stable since it has not been possible to establish the convergence of η to zero. Thus, the above analysis only guarantees boundedness of the parameter errors, not parameter convergence.

Now, consider a forcing function $r(t)$ having the following properties: (i) it is a smooth function; (ii) $r(t)$ and all its time derivatives are bounded; (iii) it satisfies a "finite energy" condition,

$$\int_0^\infty |r(t)|^2 \, \mathrm{d}t < \infty; \tag{20}$$

and (iv) $r(t) \to 0$ as $t \to \infty$. In particular, for the purpose of this analysis, choose the function $r(t)$ as follows

$$r(t) = -k^2\, 2(x_p^{\mathrm{T}} P_x b) d_0, \tag{21}$$

where k is an arbitrary constant. Referring to Eq. (17), once again $\dot{V}$ is negative semi-definite, and the previous sequence of arguments goes through entirely. The conclusion, once again, is the same; namely, the plant states x_p and the output error e are both guaranteed to converge to zero. However, as before, the analysis only shows parameter error η to be bounded; convergence of η to zero may possibly be achieved by use of a suitable persistently exciting forcing function $r(t)$, but this is not guaranteed.

An analysis that explicitly accounts for a *persistently exciting* forcing $r(t)$ and provides a stronger result, including conditions under which parameter convergence may be obtained, has not yet been achieved. Nevertheless, the above analysis is useful in two ways. First, it reveals that a suitable choice of $r(t)$ can provide an additional negative semi-definite term to $\dot{V}$. When compared with the unforced case, this may result in, (i) faster convergence of e, x_p; and (ii) lower values of $V(t \to \infty)$, and hence better convergence of the parameter errors. Second, the form of $r(t)$ in Eq. (21) suggests that a suitable choice for the forcing function would be a sinusoidal signal modulated by a function that is exponentially decreasing with time. Simulation of the closed-loop response of the system in Fig. 2 in the following sections with such a forcing function reveals that partial parameter convergence is indeed achieved.

4. Baseline study

In the light of the above discussion, the forcing function $r(t)$ is chosen to be of the form

$$r(t) = r_0 \sin(\Omega t) \exp(-t/T) \tag{22}$$

with baseline values of $r_0 = 0.01$, $\Omega = 0.2$, and $T = 300$. Note that the variable t refers to a nondimensional time. The matrix Γ in Eq. (15) is taken as

$$\Gamma = \mathrm{diag}(0.1, 0.01, 0.001, 0.001, 0.001) \tag{23}$$

As in Ref. [8], $d_0 = 1$ is assumed without loss of generality. Initial conditions on the plant and model states are as specified in Section 2 on open-loop response. The controller parameters θ_i are all taken to be zero initially. With these choices, results from the closed-loop simulation of the system in Fig. 2 are described below.

Fig. 3 shows the plant states, x_{p_1}, x_{p_2}, tending to zero with time, and Fig. 4 shows the 2-norm of the output error vector[1] also converging to zero. Thus, tracking and control have both been successfully achieved. This, by itself, is not remarkable as it is well known that both tracking and control can be obtained even without the use of a forcing function, as has been demonstrated in Refs. [8,11]. Of greater interest are Figs. 5 and 6 which show that the linear parameter errors, η_1, η_2, also converge to zero. That is, the controller parameters, θ_1, θ_2, actually converge to their

[1]For purposes of economy and following the usual practice of showing the norm of the error, the 2-norm has been plotted in Fig. 4, even though e contains both displacement and velocity error terms with equal weighting. It has, however, been confirmed that individual elements of the error vector do tend to zero satisfactorily.

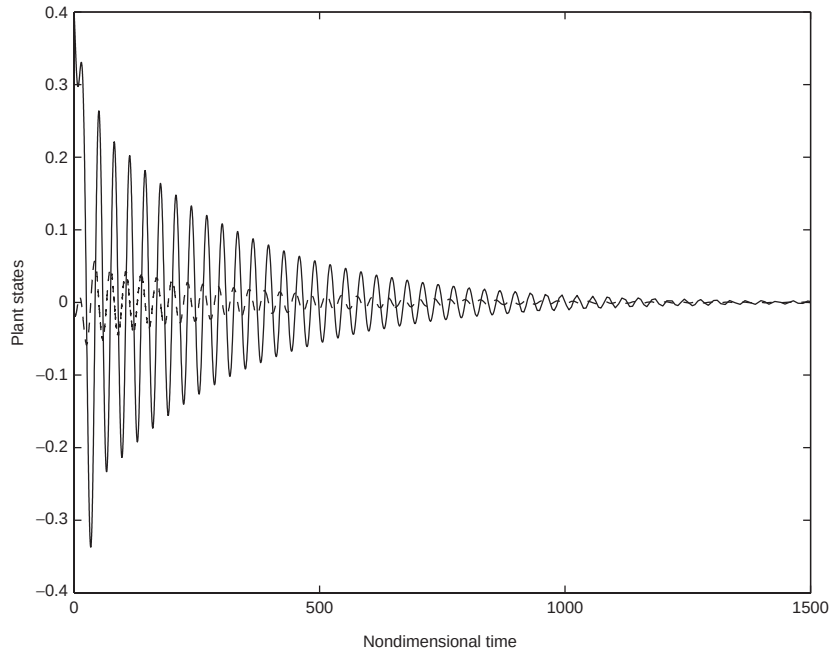

Fig. 3. Closed-loop response of the system in Fig. 2 showing convergence of plant states (x_{p_1}: —; x_{p_2}: - -).

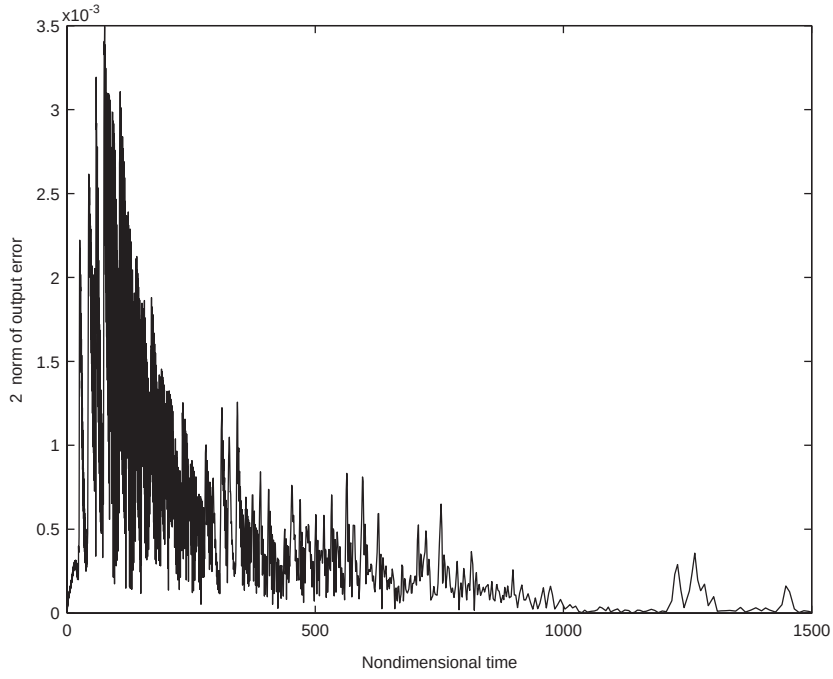

Fig. 4. Closed-loop response of the system in Fig. 2 showing convergence of error, e, between the plant and model outputs.

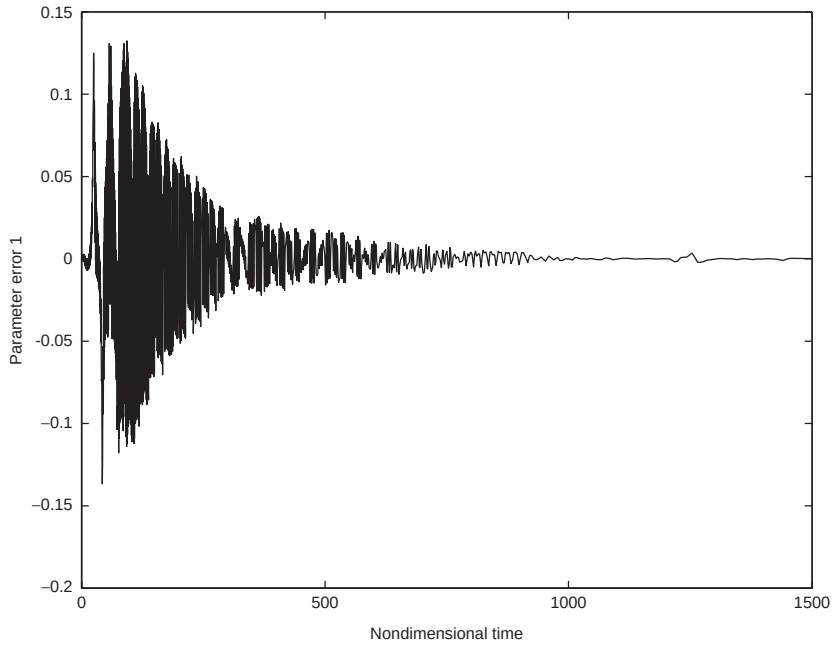

Fig. 5. Closed-loop response of the system in Fig. 2 showing convergence of the linear parameter error, η_1.

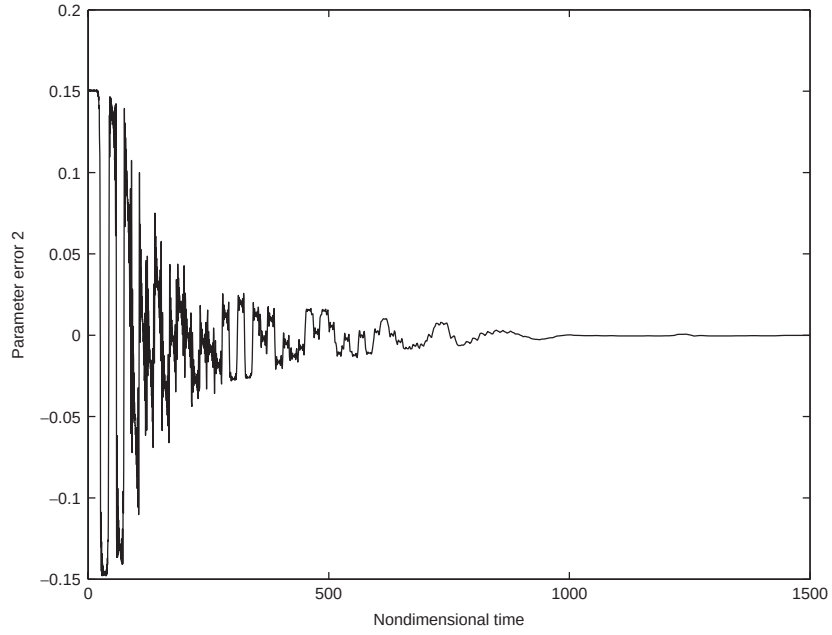

Fig. 6. Closed-loop response of the system in Fig. 2 showing convergence of the linear parameter error, η_2.

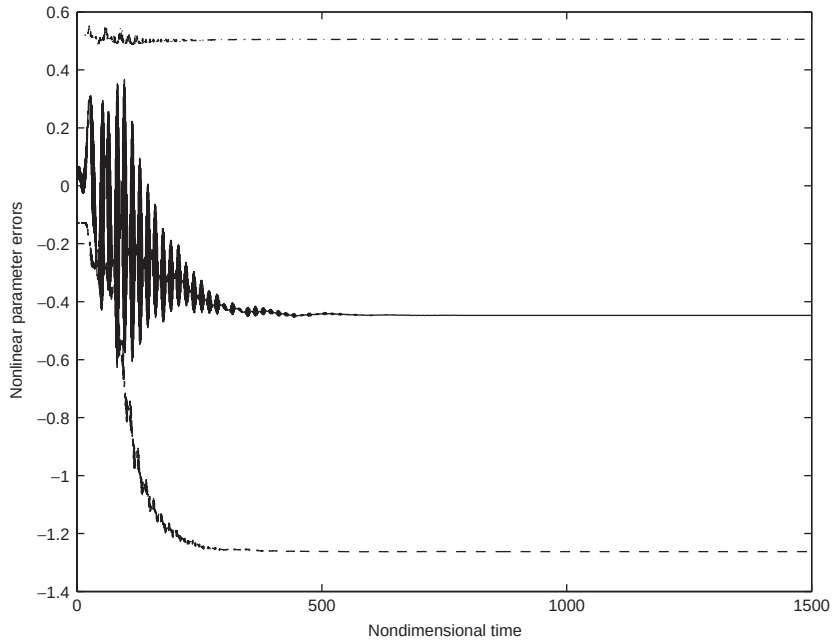

Fig. 7. Closed-loop response of the system in Fig. 2 showing non-convergence of the nonlinear parameter errors (η_3: —; η_4: - -; η_5: - . -).

ideal values, θ_1^*, θ_2^*, defined in Eq. (7). However, it is seen in Fig. 7 that the nonlinear parameter errors, η_3, η_4, η_5, do not converge to zero. Hence, the parameters, $\theta_3, \theta_4, \theta_5$, do not converge to their ideal values as given in Eq. (7). The adaptive feedback linearization scheme employed in this study, therefore, provides estimates of the linear plant parameters, θ_1, θ_2, but not of the nonlinear parameters.

It is instructive to understand why convergence of the nonlinear parameter errors was not achieved in Fig. 7. For this, consider the nonlinear terms in Eq. (4) for the closed-loop plant dynamics. The sum of these three terms, denoted by the symbol S, is as follows

$$S = (c_1 a_3 - d_0 \theta_3) x_{p_1}^3 + (c_1 a_4 - d_0 \theta_4) x_{p_1}^2 x_{p_2} + (c_1 a_5 - d_0 \theta_5) x_{p_1} x_{p_2}^2. \tag{24}$$

In each of the bracketed expressions in Eq. (24), the first term is due to the open-loop plant dynamics in Eq. (1) and the second term is from the control law in Eq. (3). A plot of the variation of S during the closed-loop response of the system is shown in Fig. 8; it can be seen that S converges to zero. However, as seen from Fig. 7, the non-convergence of the nonlinear controller parameters implies that each of the bracketed expressions in Eq. (24) is not individually eliminated. Instead, the sum of all nonlinear terms in the open-loop plant dynamics is collectively canceled by an equal and opposite contribution from the controller.

It can be seen from Fig. 8 that S effectively settles down to zero for $t \approx 600$. The nonlinear parameters also stop evolving at about the same time and the closed-loop plant dynamics is then essentially linear. The linear parameter errors in Figs. 5 and 6 continue to be driven until they apparently converge to zero at some $t > 1000$. At that point, model matching between the closed-loop plant dynamics and the reference model is effectively achieved. Subsequently, Figs. 3 and 4

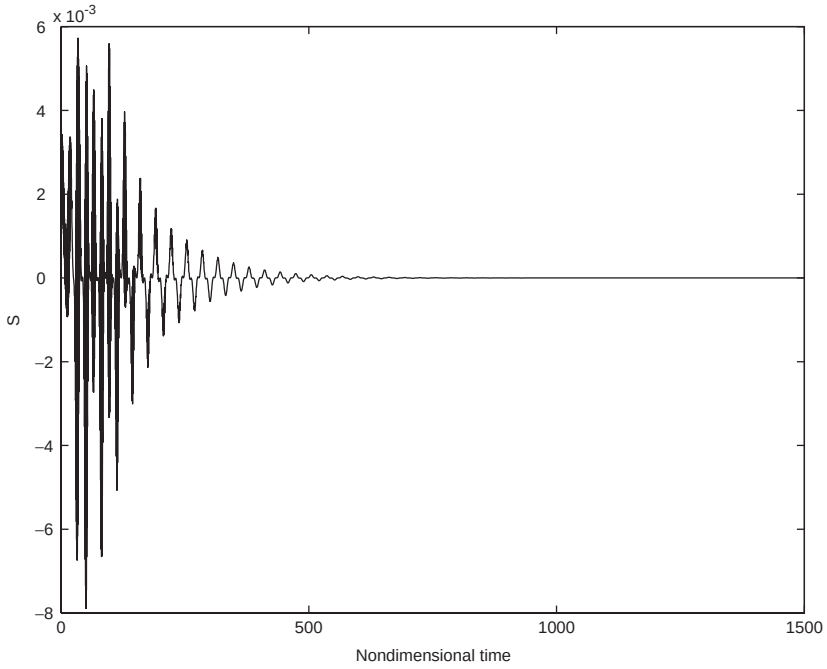

Fig. 8. Closed-loop response of the system in Fig. 2 showing convergence of the variable, S, defined in Eq. (24).

show that the plant states, x_p, and the output error, e, respectively tend to zero by $t \approx 1500$, and so does the control input, u, as seen in Fig. 9. Thus, once $S = 0$, there is no significant effect driving the nonlinear parameters towards their ideal values, and hence parameter convergence is obtained only for the linear parameters.

4.1. Comparison with unforced case

It is worthwhile to contrast the performance of the adaptive feedback linearization scheme with forcing, especially the parameter convergence observed in Figs. 5 and 6, with the results obtained from a similar procedure, but without a forcing function. While tracking and regulation are achieved even in the unforced case, Figs. 10 and 11 show that neither of the linear parameter errors converges to zero; hence, no parameter estimation is possible. The difference between the forced and unforced systems can be understood by considering Fig. 12, which shows a plot of the natural logarithm of V, the Lyapunov function in Eq. (15), for both the forced and unforced cases, with all other parameters held at their baseline values. It can be noticed that Fig. 12 shows a lower value of $\ln V$ for the forced case. This can be attributed to the smaller value of the quadratic parameter error term in Eq. (15), and is therefore directly related to the successful parameter convergence observed in Figs. 5 and 6 for the forced case. The forcing function, therefore, drives the parameter errors to lower values; however, as explained earlier, it is unable to drive the nonlinear parameter errors individually to zero.

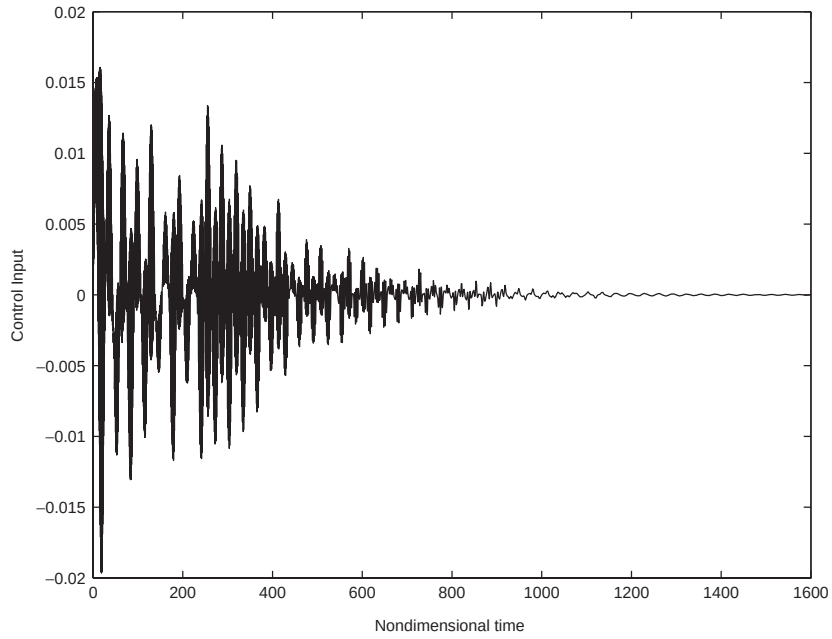

Fig. 9. Closed-loop response of the system in Fig. 2 showing variation of control, u, with time.

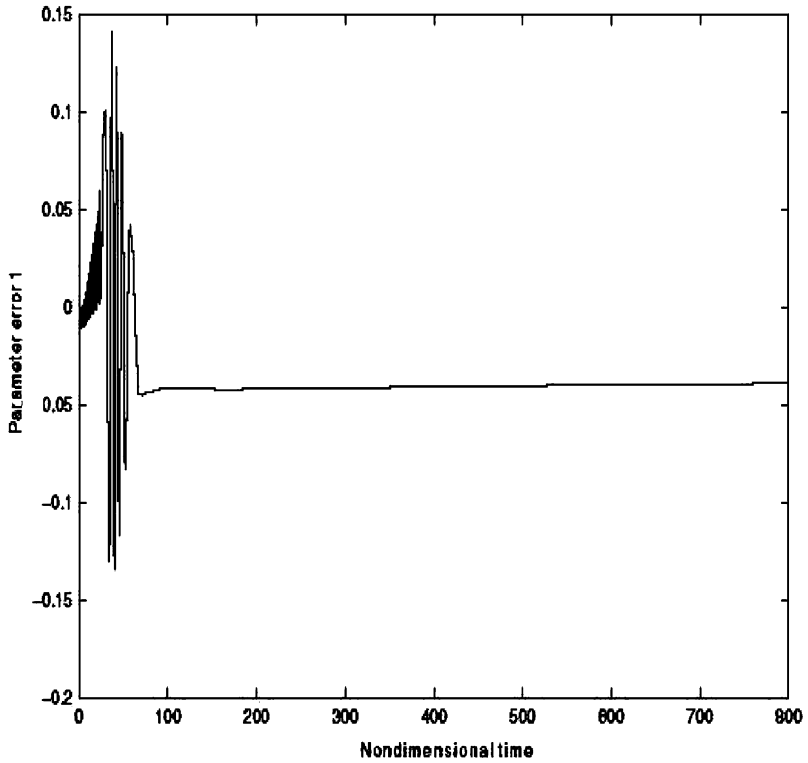

Fig. 10. Closed-loop response of the system in Fig. 2 without the forcing $r(t)$ showing non-convergence of the linear parameter error, η_1.

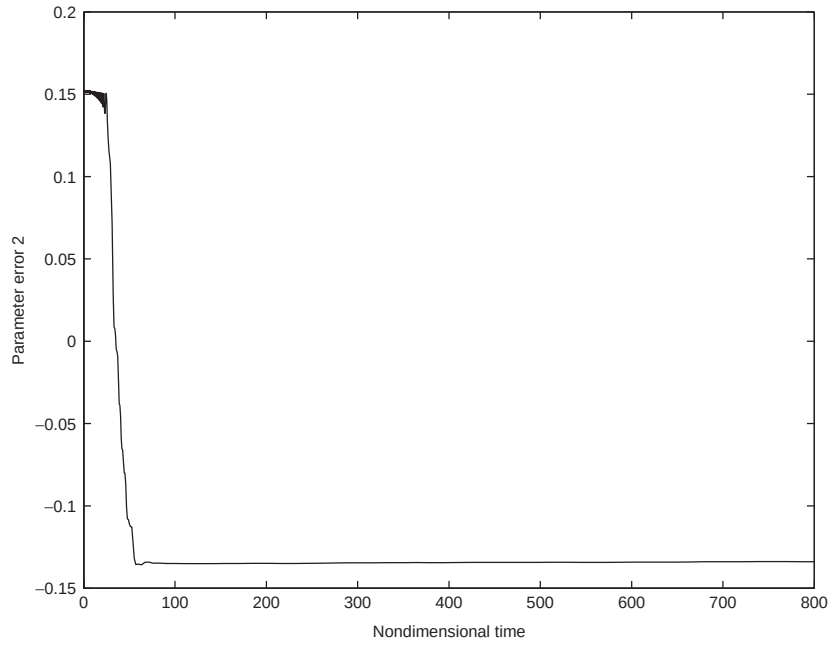

Fig. 11. Closed-loop response of the system in Fig. 2 without the forcing $r(t)$ showing non-convergence of the linear parameter error, η_2.

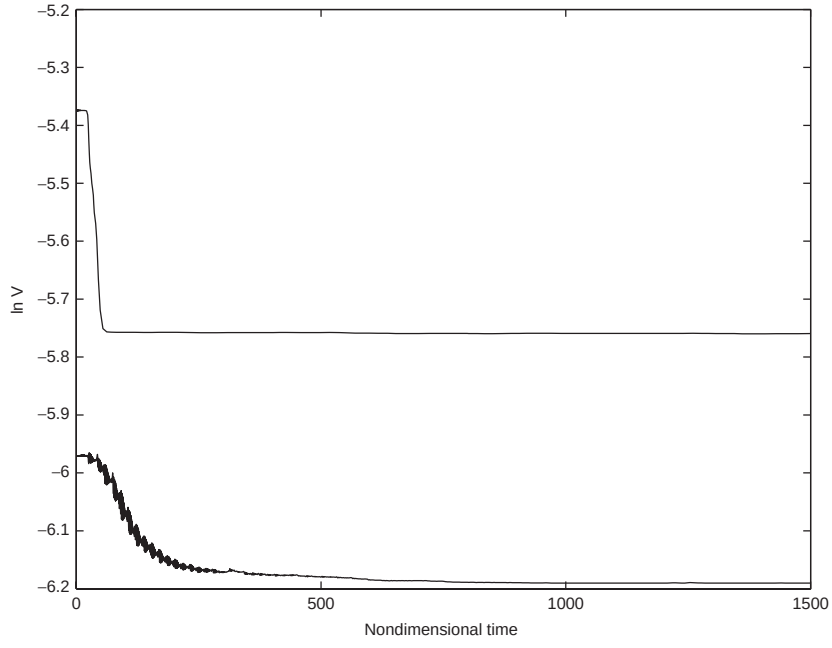

Fig. 12. Variation of ln V as a function of time for both forced and unforced response of the closed-loop system in Fig. 2 (forced: lower graph; unforced: upper graph).

5. Parametric study

It is of interest to examine whether a different choice of any of the constants in the adaptive feedback linearization scheme has an effect on the parameter convergence. The various constants in question are: (i) the amplitude, frequency, and decay time of the forcing function in Eq. (22); (ii) the diagonal elements of the Γ matrix in Eq. (23), and (iii) the Q_e, Q_x matrices, and hence the elements of the corresponding P matrices in Eq. (19). All the constants listed above were systematically varied, one at a time, while keeping all the other constants fixed at their baseline values. Following the standard practice, typical variations of the constants considered were from 0.5 to 2.0 times their values in the baseline study. In every case, results of the closed-loop simulation showed no qualitative difference from what was observed in the baseline study, thereby indicating that the results are unaffected under reasonable changes in the parameter values. Tracking, regulation, and convergence of the linear parameters was achieved in all cases, while the nonlinear parameters did not converge. Numerically, there were minor differences in the time taken for S, the linear parameter errors, and the tracking error to converge to zero. Of greater significance is the value of $\ln V$ to which the system converged when the constants in the forcing function were varied. It can be seen from Figs. 13–15 that larger amplitude, higher frequency, and greater decay time, all contribute to a lower value of $\ln V$, and hence smaller parameter errors (for the nonlinear parameters since the linear parameters converge to zero anyway). However, additional simulations have shown that this trend is not sustained for arbitrary variation of the forcing function parameters, and it is therefore not possible to reduce the nonlinear parameter

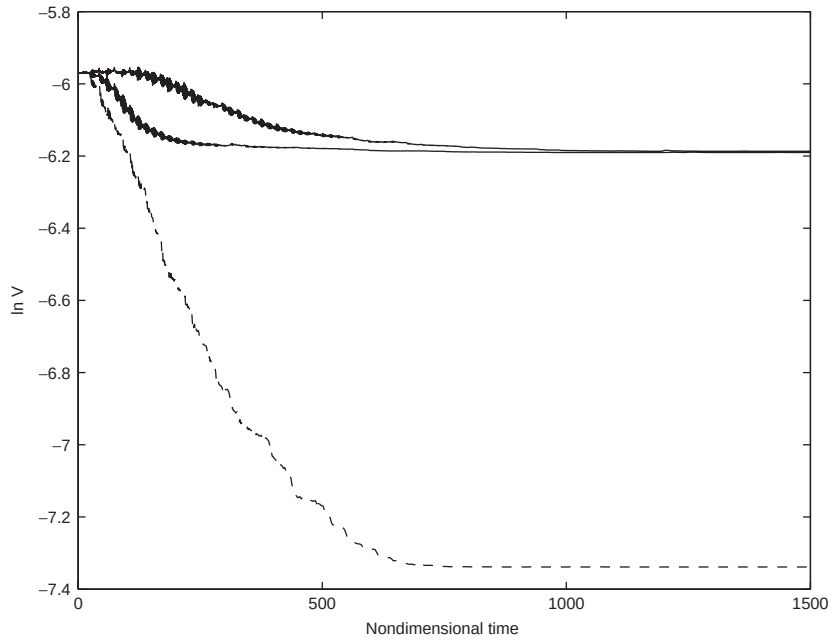

Fig. 13. Variation of $\ln V$ as a function of time for different values of r_0, the amplitude of the forcing function ($r_0 = 0.005$: — (upper graph); $r_0 = 0.01$: — (lower graph); $r_0 = 0.02$: - - -).

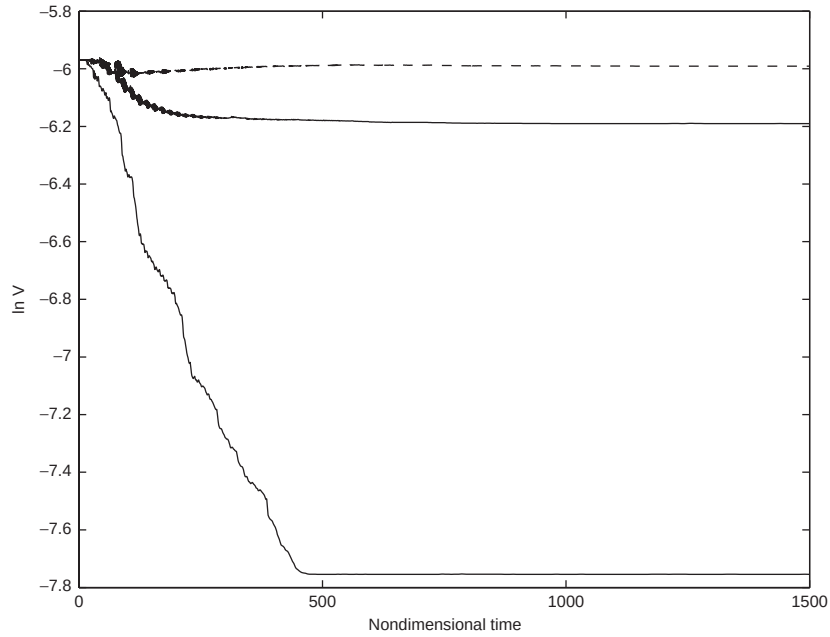

Fig. 14. Variation of ln V as a function of time for different values of Ω, the frequency of the forcing function ($\Omega = 0.1$: - - -; $\Omega = 0.2$: — (upper graph); $\Omega = 0.4$: — (lower graph)).

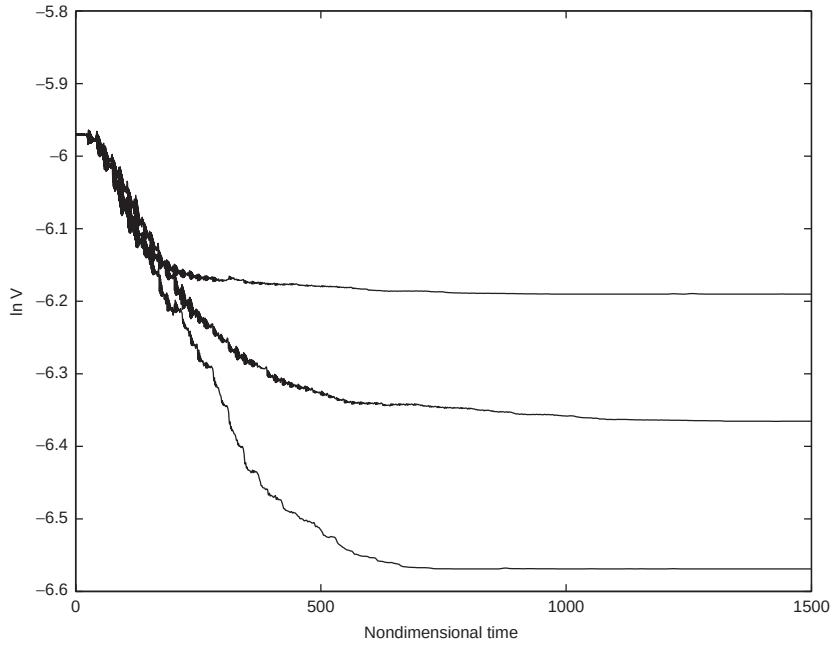

Fig. 15. Variation of ln V as a function of time for different values of T, the decay time of the forcing function ($T = 208$: upper graph; $T = 300$: middle graph; $T = 416$: lower graph).

errors to zero in this manner. No attempt was made to look for optimal values of these parameters as that was not of interest to this study.

6. Effect of measurement noise

In practice, the adaptive feedback linearization scheme in Fig. 2 would have to perform even when the plant outputs y_p are corrupted by measurement noise. The experimental work in Ref. [11] has established that control of limit cycling motion can be successfully achieved in the presence of measurement noise. It remains to be seen whether tracking and parameter estimation are still possible when measurement noise is present. For this purpose, a measurement noise signal, as suggested in Ref. [7], is considered in the plant output, Eq. (2), as follows

$$\delta y_1 = 0.003 \sin(10t), \quad \delta y_2 = 0. \tag{25}$$

The baseline study of the closed-loop system in Fig. 2 is now repeated with the noise signal in Eq. (25) incorporated in the plant output. Fig. 16 is a plot of the 2-norm of the output error showing that tracking, though understandably not perfect, is substantially achieved. It can be seen from Figs. 17 and 18 that the linear parameter errors in this case do converge to zero in a statistical sense. Thus, parameter estimation of the linear parameters is successful even in a noisy measurement environment. Clearly, other representations of the noise signal are possible, and it would be interesting, though beyond the scope of this work, to verify that the present method is equally effective in their presence.

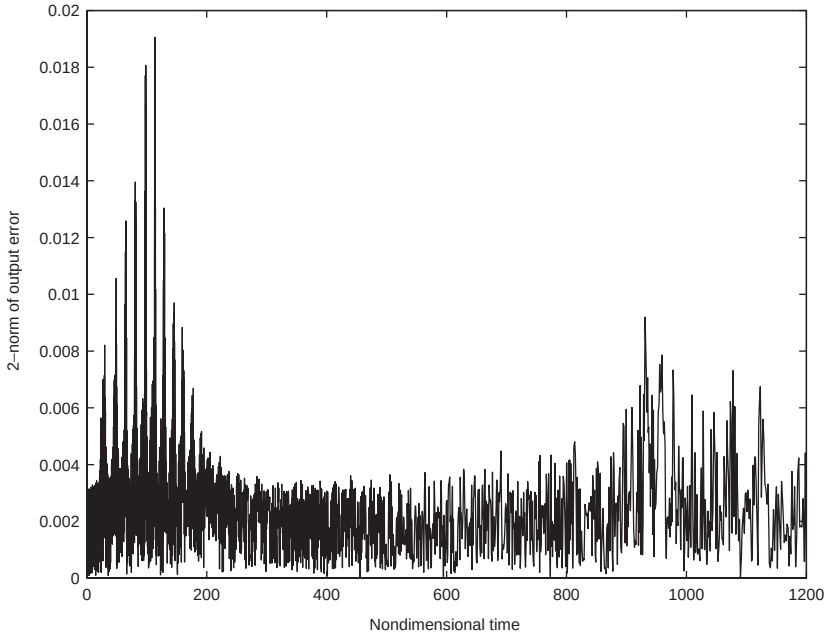

Fig. 16. Closed-loop response of the system in Fig. 2 with measurement noise showing convergence of error e, between the plant and model outputs.

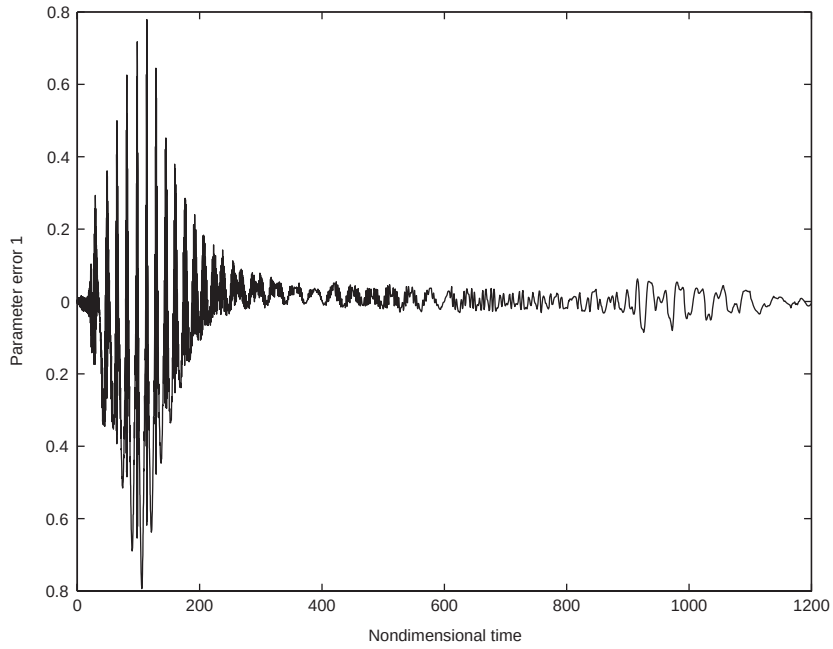

Fig. 17. Closed-loop response of the system in Fig. 2 with measurement noise showing convergence of the linear parameter error, η_1.

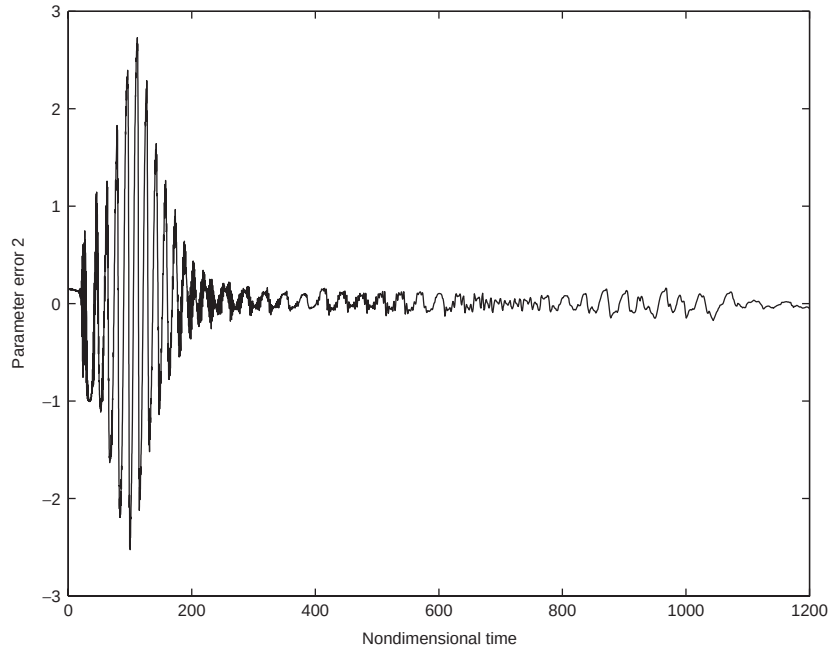

Fig. 18. Closed-loop response of the system in Fig. 2 with measurement noise showing convergence of the linear parameter error, η_2.

7. Conclusions

Parameter estimation for an unstable, limit cycling system has been successfully demonstrated using an adaptive feedback linearization scheme. Since it is well known that parameter convergence requires external forcing, a novel adaptation law has been derived by carrying out a Lyapunov analysis for the stability of the closed-loop system including a forcing function. The stability analysis itself reveals the desired form of the forcing to be an exponentially damped sinusoidal signal. Baseline simulations showing successful control, tracking, and linear parameter convergence have been reported, while the non-convergence of the nonlinear parameters has been explained. Further simulations have been carried out to compare the baseline results with those in the unforced case, where parameter convergence is not obtained, and to study the effect of varying the constants in the forcing function on parameter convergence. Finally, the baseline results, including linear parameter convergence, are shown to be successfully reproduced even in the presence of measurement noise in the plant output signal.

The example of limit cycle oscillations in delta wing roll dynamics has been considered as a typical case; however, the procedure described in this paper may be easily applied to other systems of a similar nature. Clearly, the choice of a linear reference model as in Eq. (5) can be made independent of the nonlinear terms in the plant model, and a suitable feedback linearizing control as in Eq. (3) can be derived for a wide class of nonlinear systems. Likewise, an adaptation law of the form Eq. (16) can be obtained—the elements of the vector $h(x_p)$ will vary depending on the nonlinear terms in the plant model—and the Lyapunov analysis can then be carried out along similar lines as shown in this paper.

The issue of devising an adaptation law and a suitable, possibly persistently exciting, forcing signal, which will also guarantee convergence of the nonlinear parameters, remains a subject for future work.

Acknowledgements

The authors would like to acknowledge useful discussions with Dr. S.P. Bhat and, in particular, his suggestion for the form of Eq. (21) and the subsequent stability analysis.

References

[1] S.H. Strogatz, *Nonlinear Dynamics and Chaos*, Addison-Wesley, Reading, MA, 1994, pp. 196–240.
[2] N. Ananthkrishnan, K. Sudhakar, S. Sudershan, A. Agarwal, Application of secondary bifurcations to large amplitude limit cycles in mechanical systems, *Journal of Sound and Vibration* 215 (1) (1998) 183–188.
[3] N. Ananthkrishnan, S. Sudershan, K. Sudhakar, A. Verma, Large amplitude limit cycles in resonantly coupled oscillators, *Journal of Sound and Vibration* 231 (5) (2000) 1377–1382.
[4] R.D. Nowak, Nonlinear system identification, *Circuits, Systems, and Signal Processing* 21 (1) (2002) 109–122.
[5] M. Thothadri, R.A. Casas, F.C. Moon, R. D'Andrea, C.R. Johnson, Nonlinear system identification of multi-degree-of-freedom systems, *Nonlinear Dynamics* 32 (3) (2003) 307–322.
[6] R.V. Jategaonkar, *Lecture Notes, Short Course on Flight Vehicle System Identification in Time Domain*, Indian Institute of Technology (Bombay), Mumbai, India, January 19–21, 2004.

[7] J.-J.E. Slotine, W. Li, *Applied Nonlinear Control*, Prentice-Hall, Englewood Cliffs, NJ, 1991, pp. 311–391.
[8] S.N. Singh, W. Yim, W.R. Wells, Direct adaptive and neural control of wing rock motion of slender delta wings, *Journal of Guidance, Control, and Dynamics* 18 (1) (1995) 25–30.
[9] M.M. Monahemi, M. Krstic, Control of wing rock motion using adaptive feedback linearization, *Journal of Guidance, Control, and Dynamics* 19 (4) (1996) 905–912.
[10] C. Hsu, C.E. Lan, Theory of wing rock, *Journal of Aircraft* 22 (10) (1985) 920–924.
[11] S.D. Vaidya, N. Ananthkrishnan, Adaptive control of delta wing rock in stability wind tunnel, *Journal of the Aeronautical Society of India* 49 (4) (1997) 183–187.
[12] K.S. Narendra, A. Annaswamy, *Stable Adaptive Systems*, Prentice-Hall, Englewood Cliffs, NJ, 1989, pp. 238–269.
[13] M. Krstic, I. Kanellakopoulos, P.V. Kokotovic, *Nonlinear and Adaptive Control Design*, Wiley, New York, 1995.
[14] J.T. Huang, Sufficient conditions for parameter convergence in linearizable systems, *IEEE Transactions on Automatic Control* 48 (5) (2003) 878–890.
[15] R.V. Jategaonkar, F. Thielecke, Evaluation of parameter estimation methods for unstable aircraft, *Journal of Aircraft* 31 (2) (1994) 510–519.
[16] S.M. Savaresi, R.R. Bitmead, J.J. Dunstan, Nonlinear system identification using closed-loop data with no external excitation: the case of a lean combustion chamber, *International Journal of Control* 74 (18) (2001) 1796–1806.
[17] A.H. Nayfeh, J.M. Elzebda, D.T. Mook, Analytical study of the subsonic wing rock phenomenon for slender delta wings, *Journal of Aircraft* 26 (9) (1989) 805–809.
[18] J.M. Elzebda, A.H. Nayfeh, D.T. Mook, Development of an analytical model of wing rock for slender delta wings, *Journal of Aircraft* 26 (8) (1989) 737–743.
[19] D. Levin, J. Katz, Dynamic load measurements with delta wings undergoing self-induced roll oscillations, *Journal of Aircraft* 21 (1) (1984) 30–36.
[20] K. Huseyin, *Vibrations and Stability of Multiple Parameter Systems*, Sijthoff and Noordhoff, Alphen aan den Rijn, The Netherlands, 1978, p. 47.